Homoepitaxial growth of alumina films on NiAl(110) using NO_2

THESIS

submitted in partial fulfillment of the
requirements for the degree of

BACHELOR OF SCIENCE
in
PHYSICS

Author : Joost Vermeer
Student ID :
Supervisor : Irene Groot
2^{nd} corrector : Tjerk Oosterkamp

Leiden, The Netherlands, January 17, 2019

Homoepitaxial growth of alumina films on NiAl(110) using NO_2

Joost Vermeer

Huygens-Kamerlingh Onnes Laboratory, Leiden University
P.O. Box 9500, 2300 RA Leiden, The Netherlands

January 17, 2019

Abstract

In the search for substrates used in the investigation of catalytic nanoparticles we have grown alumina films on NiAl(110) past 5.35 Å, the maximum thickness that can be obtained with molecular oxygen [1]. A NiAl(110) sample was first oxidized to that thickness with molecular oxygen, after which it was stepwise oxidized with NO_2. The film thickness, crystal structure and chemical composition were measured using Low Energy Electron Diffraction (LEED), X-ray Photoelectron Spectroscopy (XPS) and Scanning Tunneling Microscopy (STM). We have confirmed that film grown with NO_2 follows the theoretical model of Cabrera and Mott[2][3] up to 6.9 Å. STM images show an increase in the number of islands and vacancies in the metal, indicating that this growth happened at the film-metal interface and not the film surface.

Contents

Chapter 1

Introduction

In their attempt to find ever better catalysts, chemical companies have turned to nanoparticles. These particles have many properties that their bulk states do not have, like special facets and a high surface to mass ratio. To use them in an industrial setting they need to be placed on a support, or they would be carried away by the flow of the the gas or liquid it is reacting with. One of the most common used supports is aluminum oxide, also called alumina. It is strong, cheap and chemically inert, which makes it ideal in situations where one does not want any uncontrolled reactions happening.

Our group investigate these industrial catalytic processes. We try to mimic the industrial circumstances as close as possible, but unfortunately that is not possible in this case. Bulk alumina is hard to investigate in an academic setting since research groups cannot use one of their most important measurement methods, Scanning Tunneling Microscopy (STM). An STM setup consists of a conducting tip which is about a nanometer away from the surface. If the surface is conducting, a voltage difference between the tip and the sample creates a tunneling current. This tunneling current is measurable and depends on both the distance between the tip and the sample, as well as the electronic state of the surface. But if the sample is an electrical insulator this is impossible, since there is no low potential area for the electrons to tunnel to.

Since alumina itself is an insulator a conducting support is needed to investigate nanoparticles on alumina. This can be done by oxidizing a NiAl crystal and placing the nanoparticles on top of the alumina film that is formed by the oxidation. This system, alumina films on single crystal nickel-aluminum, is widely studied by surface scientists [1][4][5]. It is strong and chemically inert like bulk alumina, and it has a well-defined

crystal structure. The film has a limited growth in molecular oxygen, since the energy for oxygen adsorption comes from electrons tunneling from the metal to the film surface. In thicker films the tunneling current decreases which lowers the energy available at the surface. At a certain point adsorption is no longer thermodynamically favored and the film stops growing.

Molybdenum oxide nanoparticles

A system that was previously studied by our group was MoO_3 nanoparticles on an O_2 limited alumina film [6] and their catalytic behavior in the desulfurization of sulfur-containing hydrocarbons. When investigating the MoO_3 nanoparticles it was discovered that the molybdenum was reduced to metal and the alumina film thickness was increasing. This could only be explained by assuming that the MoO_3 dissociates, with the oxygen atoms moving into the alumina film, increasing its thickness.

In order to further investigate this system we need to prevent the dissociation of the molybdenum oxide. Since the energy required for the dissociation originates from the electrons tunneling through the metal, and the tunneling current depends on the thickness of the film barrier, a thicker film will reduce the energy available for dissociation. If the film is thick enough, the amount of energy available at the surface will be so low that the oxygen atoms remain within the molybdenum oxide. At such a thickness the molybdenum oxide and the desulfurization of sulfur-containing hydrocarbons can be investigated as if we were investigating the bulk alumina.

There is one important condition for this to work. We still have to be able to scan the surface with STM. Since the alumina is an insulator the electrons have to tunnel through the film as well. The thicker the film is, the larger the distance between the tip and the NiAl support. This decreases the tunneling current and lowers the signal to noise ratio. To prevent that we could move closer the tip is to the alumina surface, but doing so would increase the probability that the tip crashes into the sample. It is therefore questionable whether we are able to scan on the thick films and actually investigate the nanoparticles.

There is more unknown about this plan. It is unclear which properties of the O_2 limited alumina film remain past the O_2 limit. Therefore these properties, especially the crystal structure and growth speed, need to be investigated at thicker films. It also gives us opportunities. Since the O_2 limited film is quite stable, unlike the thinner films, we should be able to answer one of the open questions of Cabrera-Mott growth [2]: Where does

the film grow? This is an interesting question in itself, which we are able to investigate in this project.

In order to answer all those questions we will stepwise increase the film thickness with NO_2 while investigating the surface in between, up to the point where STM becomes almost impossible. At that point MoO_3 nanoparticles are deposited on the surface and subsequently exposed to a high pressure environment in order to test their stability.

Chapter 2

Theory

2.1 Quantitative description of oxide film growth

The first physical description of the limited oxidation behavior was written by Cabrera and Mott [2]. For very thin or ultra thin films they assume that ionic transport is the limiting growth factor. This ionic transport is caused by diffusion and affected by the electric field of the so called Mott capacitor. This Mott capacitor is created by electrons tunneling through the oxide layer to oxygen on the surface, which has empty states below the metal's Fermi level. In the case of a constant electric potential of the Mott capacitor this model leads to the following rate equation for oxide growth [2]:

$$\frac{dX}{dt} = 2u \sinh\left(\frac{X_1}{X}\right) \tag{2.1}$$

Where u is the diffusion velocity and X_1 is a characteristic length. The diffusion velocity is given by $u = u_0 e^{(W/k_b T)}$, where W is the potential energy of a diffusion location inside the film and X_1 depends on the shape of the oxide barrier, the electric potential of the Mott capacitor and the temperature.

Equation (2.1) is a differential equation which is solved by Cabrera and Mott. For thin films they knew $X_1 \gg X$, so they aproximated equation (2.1) to create their inverse-logarithmic law

$$\frac{1}{X} = A - B \ln t \tag{2.2}$$

With A and B experimental constants. Richard Ghez [3] has shown that this approximation is too rough to be meaningful, and that the proper

equation should be

$$\frac{X_1}{X} = -\ln\left(\frac{t+\tau}{X^2}\right) - \ln(X_1 u) \tag{2.3}$$

where τ is an offset needed because the Cabrera Mott Theory is invalid as long as there is not yet a full layer formed yet. We can rewrite this equation into

$$\frac{X_1}{X} = \ln\left(\frac{X^2}{X_1 u(t+\tau)}\right) \tag{2.4}$$

$$e^{X_1/X} = \frac{X^2}{X_1 u(t+\tau)} \tag{2.5}$$

$$\frac{X_1^2}{X^2} e^{X_1/X} = \frac{X_1}{u(t+\tau)} \tag{2.6}$$

$$\frac{X_1^2}{4X^2}\left(e^{X_1/(2X)}\right)^2 = \left(\frac{X_1}{2X} e^{X_1/(2X)}\right)^2 = \frac{X_1}{4u(t+\tau)} \tag{2.7}$$

$$\frac{X_1}{2X} e^{X_1/(2X)} = \sqrt{\frac{X_1}{4u(t+\tau)}} \tag{2.8}$$

This equation can be solved, but not analytically. It requires the Lambert W function $\mathrm{W}(x)$, which is the inverse function of $x = f(y) = ye^y$. This function is in general complex and multivalued, but for $x > 0$ it has only one real-valued branch, $\mathrm{W}_0(x)$. Since we are only interested in real results we use that branch. So equation (2.8) gives

$$\frac{X_1}{2X} = \mathrm{W}_0\left(\sqrt{\frac{X_1}{4u(t+\tau)}}\right) \tag{2.9}$$

$$X = \frac{X_1}{2\mathrm{W}_0\left(\sqrt{\frac{X_1}{4u(t+\tau)}}\right)} \tag{2.10}$$

Note that in both equation (2.2) and (2.10) $dX/dt > 0$ for all t, so according to this model, the film should never stop growing. Cabrera and Mott acknowledge this, but they do not provide a solution or an explanation. They just assume that when film thickness increases with less than 10^{-6} nm/s, the thickness increases so little that we can assume it has stopped increasing.

2.2 Qualitative description of oxide film growth

While the Cabrera-Mott theory gives a good quantitative description, it does not give a good qualitative description. Even worse, we know some assumptions made in the theory are wrong. At the start the theory assumes that there is atomic oxygen on the surface, but there is no explanation how it arrived there. Since atomic oxygen gas is extremely rare and thermodynamically unstable, we assume that it deposited on the surface by some oxygen containing gas. Cabrera and Mott do not address that nor ask the question what influence the type of oxygen containing gas has on the film growth. Additionally it is not taken into account that the oxide film is made out of atoms, which means that the film can only have a discrete thickness and it might not grow uniformly. These considerations are taken into account by Baran et al [7] who have investigated the oxidation of Al(111).

It all starts at the clean metal surface, which is NiAl(110) in our case. When molecular oxygen is introduced to the metal the oxygen quickly reacts with the metal surface and creates a film one monolayer thick. This layer acts as a barrier for the oxygen molecules that arrives later.

The molecular oxygen that arrives after the first layer is formed is attached to the newly formed oxide surface by partial dissociative adsorption, as shown in figure 2.1. The oxygen molecule breaks up one of its molecular bonds and bonds to one or more aluminum atoms in the oxide. This costs energy, which is provided by electrons tunneling from the metal surface to oxygen. When the electrons are captured by the oxygen they enter a lower energy state and thus release energy. How much energy is released depends on the atom and the chemical composition, this is called the electron affinity. The net change in energy is called the adsorption energy, and needs to be negative to make the reaction thermodynamically favorable.

The electrons which are tunneling through the film create a second effect, which was already described by Cabrera and Mott. They create a negative charge conjugation at the surface and a positive charge conjugation at the interface[8]. This Mott capacitor creates an electric field inside the oxide, which enhances the diffusion of ions through the film.

One of the main questions of this thesis is what happens after the oxygen dissociation. There are two equally valid options, which are shown in figure 2.2. Either the oxygen ions diffuse through the film to form a new film layer at the film-support interface, or the aluminum atoms in the support form aluminum ions which diffuse through the film to oxidize and form a new film layer at the surface. If the film grows at the inter-

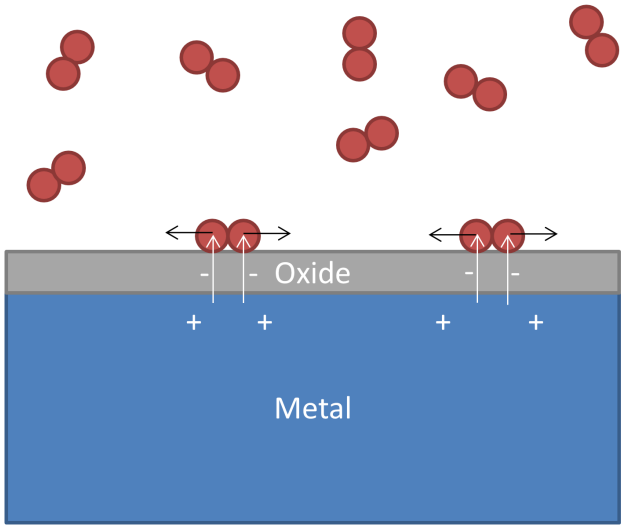

Figure 2.1: *The Mott capacitor is created electrons are tunneling through the film to be captured by the oxygen. The energy released by this process allows the molecular oxygen to partially dissociate and bond to the oxide.*

face, there would be extra atoms between the support and the film, which cause lattice strain and bulging in the film. If the film grows at the surface, we expect many small islands to be formed, which will have merged into larger ones after annealing. The first option will create a curved surface without steps, while the second option creates many steps. Cabrera and Mott assumed the second option was true, but they did not give any conclusive evidence for it. This is copied by many others, but so far we have not yet seen any conclusive experimental evidence by anybody.

The thicker the film is, the wider the tunnel barrier, and the lower the tunnel current. This decreases the charge conjugation on both the surface and the interface and thus the electric field of the Mott capacitor. This lowers the electric force on the ions, which lowers the diffusion speed, which lowers the film growth according to Cabrera and Mott's assumption. It does not stop it, though. The fact that the film completely stops growing is due to a second effect [7]. The lower tunnel current decreases the amount of electrons that are captured by the oxygen. Because the electron affinity is fixed, less captured electrons means less energy available for oxygen dissociation, increasing the adsorption energy. When the tunnel current becomes too low, the adsorption energy becomes positive and adsorption is no longer thermodynamically favored. The exact thickness at which this happens depends not only at the oxidizer's electron affinity, but also on the gas pressure [9]. That is because the Gibbs free energy de-

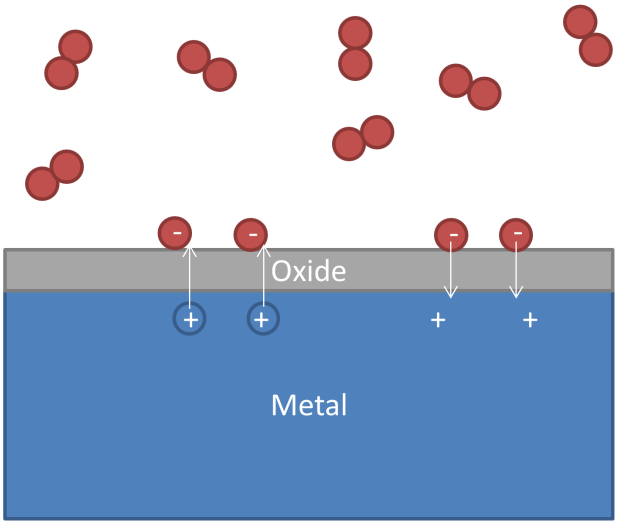

Figure 2.2: *The two diffusion methods: Either the aluminum ions move towards the surface (as seen on the left) or the oxygen ions move towards the film-metal interface (as seen on the right).*

pends on that gas pressure. When the oxygen is adsorbed at the surface a part of that energy is released, lowering the adsorption energy.

For alumina films on NiAl(110) in 10^{-6} mbar molecular oxygen the thickness limit is 2 monolayers [1]. As we have seen in section 1, that is not enough to keep the MoO_3 oxidized in high pressure conditions. So we need to increase the thickness past the 2 monolayers limit, since thicker films decrease the ion diffusion through the film and therefore reduce the speed of the reaction. Since thickness limit only depends on the adsorption energy, we know we have to either increase the gas pressure, increase the temperature, switch to an oxidizer with either a higher electron affinity or a lower bond dissociation energy [10]. Increasing the gas pressure is easily possible, but only effective at lower pressures, since the pressure effect is mostly caused by having empty surface sites which do not exist at higher pressures. When we increase the temperature we lose the crystallinity of the film [11].This leaves us with changing the oxidizer. We have chosen NO_2, because its electron affinity is five times higher, while its bond dissociation energy is lower than that of molecular oxygen [12][13].

Chapter 3

Experimental Methods

3.1 Equipment

All the experiments discussed in this thesis were performed at the Sputnik setup in the Kamerlingh-Onnes laboratory. This setup, consists of three linked UHV vacuum chambers, an XPS chamber in the front, a preparation and LEED chamber in the center and an STM chamber in the rear [14]. The 3 vacuum chambers can be sealed off from each other, which allows us to only expose the center chamber to the oxygen, keeping the other chambers at 10^{-9} to 10^{-10} mbar. This not only allows us to more strictly control the oxidation of the sample, but it also prevents interference from the degassing oxygen and NO_2 during the measurements.

To investigate our sample we used the XPS, LEED and STM on this machine. XPS or X-ray Photoelectron Spectroscopy allows us to determine the chemical composition of the top part of our sample by targeting the sample with a monochromatic 1487 eV X-ray beam. This produces electrons via the photoelectric effect, which are measured by a detector. Most electrons from the bottom of the sample are attenuated by the atoms above, so only the signal depends heavily on the composition of the surface. This allowed us to measure the thickness of the film as shown in section 3.5.

The Low Energy Electron Diffraction (LEED) setup consists of an electron gun shooting electron at a sample. Those electrons are scattered by the atoms in the sample and interfere with each other. These electrons are then captured by a fluorescent screen, where they create an interference pattern. Because the screen is fluorescent it emits visible light when hit by electrons, which we can capture with a camera. For crystalline samples the interference pattern matches the reciprocal lattice of the sample. If a

film or adsorbate is placed on the surface of the sample the interference pattern will produce extra spots which match the atomic structure of the film. This gives us information about the surface as a whole, allowing us to see whether the film is well-structured or not and whether its crystal structure has changed.

Scanning Tunneling Microscopy or STM is the third technique we used. STM setups consist of a single atom movable tip close to the sample surface. When a voltage is applied between the conducting sample and the tip a small tunneling current will be created. The magnitude of that current depends on the distance between the tip and the conducting part of the sample. So a feedback loop can be created to keep the tip on a fixed height above the sample while scanning the sample horizontally. That way we create a height map of the conductive surface up to atomic level. Because alumina insulates we cannot detect the film directly with STM. We can however measure the height of the NiAl underneath it. That means that we can get a good view of the Alumina-NiAl interface. This allows us to answer one of our main questions: where does the alumina film grow. Growth at the interface should be visible, growth at the surface should not.

3.2 General Approach

For our main experiment we first need a crystalline oxide film. First the metal surface is cleaned as described in section 3.3, after which it is oxidized with O_2 to the saturation point. This surface is thoroughly investigated with Low Energy Electron Diffraction, Scanning Tunneling Microscopy and X-ray Photoelectron Spectroscopy. All LEED patterns were imaged with an electron energy of 67 eV, and for the thorough XPS measurement we measured the Al2p, Ni3p, O1s, C1s and N1s peaks. If the oxide film surface is clean we can start the experiment. The surface is subsequently oxidized by NO_2 and annealed. Every two NO_2 oxidation cycles the surface has been investigated with LEED and XPS, measuring Al2p, Ni3p and O1s. After 8 and after 20 cycles we also took a more thorough XPS measurement and a STM measurement.

After 20 cycles, it was just barely possible to scan the surface with well enough resolution. Since the quality of the STM images would further decrease if we would make the film thicker, we decided to not increase the film any further. On the thick alumina film molybdenum oxide nanoparticles were deposited by evaporating molybdenum metal in an atmosphere of molecular oxygen at room temperature. Directly after an XPS spectrum is measured to see whether the particles are stable or not. In section 1 we

have seen that they are unstable on a 5.35 Åfilm, the results for the thicker films can be found in section 4.4.

For the second, smaller experiment we did the following: We started with a clean alumina film surface cleaned and oxidized with O_2 as described in 3.3. The surface is dosed with 5×10^{-7} NO_2 for 5 minutes at 650 K, a 10 times higher pressure than we do for the main experiment, and investigated by STM. After this the sample is annealed for 7 minutes at 1120 K and given a second dose of No_2, by dosing it with 5×10^{-7} NO_2 for 5 minutes at 650 K and annealing 7 minutes at 1120 K. After this it is investigated by STM again. Doing so we can see better at which location the film is growing. The STM data gathered here is therefore used in section 4.3, where we discuss the results.

3.3 Sample preparation

Our cleaning method has been based on Song and Yoshitake's[15] paper on cleaning NiAl(110):

- Once sputter for 25 minutes at 1.5 keV with 4×10^{-7} mbar Ar, followed by annealing for 50 minutes at 1300 K, and cooling down to 570 K.
- Once sputter for 15 minutes at 1.5 keV with 4×10^{-7} mbar Ar, followed by dosing 1×10^{-6} mbar O_2 for 5 minutes at 1300 K annealing for 25 minutes at 1300 K, and cooling down to 570 K. If there was a high carbon signal in the last XPS measurement, this is repeated once or twice more.
- Twice sputter for 15 minutes at 1.5 keV with 4×10^{-7} mbar Ar, followed by annealing for 30 minutes at 1300 K, and cooling down to 570 K.
- Three times sputter for 15 minutes at 1.5 keV with 4×10^{-7} mbar Ar, followed by annealing for 25 minutes at 1300 K, and cooling down to 570 K.

The crystal was oxidized using O_2 with the following method, which has been shown to create a crystalline oxide [16]:

- Once dose 5×10^{-6} mbar O_2 for 5 minutes at 570 K, increase the temperature to 1300 K for 1 second and anneal 5 minutes at 1120 K.

- Once dose 5×10^{-6} mbar O_2 for 10 minutes at 570 K and anneal 5 minutes at 1120 K.

- Once dose 1×10^{-6} mbar O_2 for 10 minutes at 570 K and anneal 5 minutes at 1060 K.

Oxidation cycles using NO_2 consist of dosing 5×10^{-8} NO_2 for 5 minutes at 650 K, after which the sample is annealed for 7 minutes at 1120 K.

The higher oxidation temperatures are necessary if we want the film to grow to its Cabrera Mott limit. If the temperature is too low, the alumina atoms used to create the film can not be replaced fast enough, and a pure nickel layer can be formed. Such a layer will stop the film growth, before its limit is reached. Cai et al [17] have shown that at 298 K the nickel layer is formed, but at 573 K it is not. So based on that we oxidize our film at 570 K.

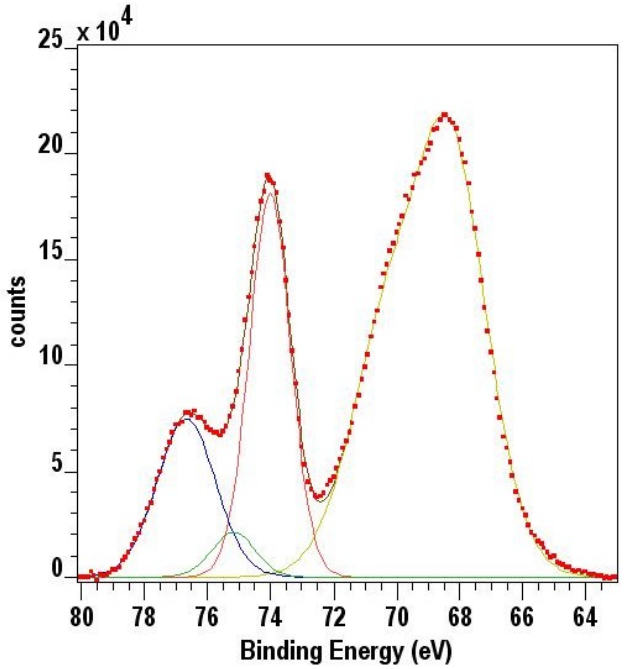

Figure 3.1: *NiAl XPS signal after 20 cycles (6000 s) of NO_2 oxidation. To improve readability the two peaks of each doublet aren't displayed separately, but only their combined contribution. The four peaks from left to right are Al2p surface, Al2p interface, Al2p bulk and Ni2p bulk.*

3.4 XPS Fitting

The XPS data is fitted using CasaXPS. All 13 measurements are fitted with the same boundary conditions: The NiAl region was fitted with 4 doublet peaks: Ni3p, Al2p bulk, Al2p interface and Al2p surface. The doublet peaks are fitted with two Gaussian-Lorentzian peaks with the same full With half Maximum. The area of the high energy peak was fixed to half of the low energy peak, since the split is due to spin-orbit coupling. For the Al2p peaks we have used the energy split used by Sharovsky et al [18], which is 0.5 eV. For the Ni3p peak no good split value could be found, so that parameter is left free.

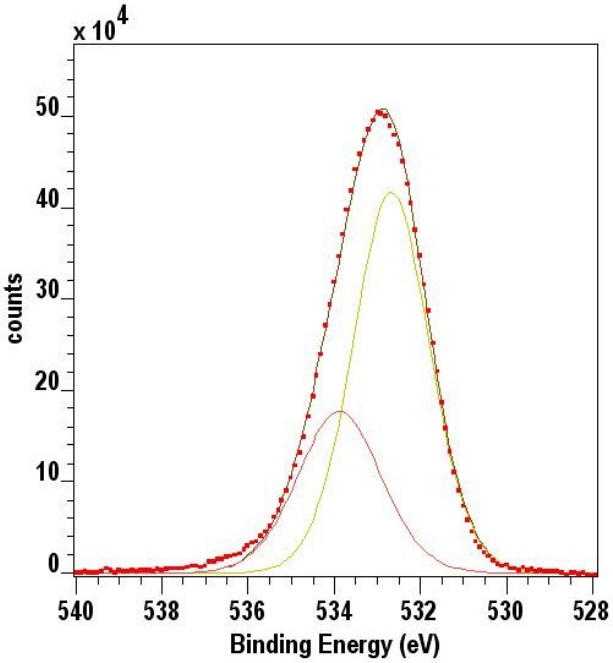

Figure 3.2: *Oxygen XPS signal after 20 cycles (6000 s) of NO_2 oxidation.*

The oxygen signal is fitted with two different peaks, with a separation of 1.2 eV. According to some [18] the high energy peak can be attributed to the surface layer and the low energy peak to the interface layer. However, others say that the surface atoms create a much stronger signal than that of the high energy peak. Martin et al [19] calculated the binding energy shifts of all 28 oxygen surface atoms in the unit cell. Their calculations show that only 8 of the oxygen surface atoms have an energy shift of 1.2 eV, which would explain the smaller size of the high energy peak. This renders any further fitting of the O1s peak useless, since we will not be able to use it in

the film thickness measurement.

3.5 XPS measurement of film thickness

According to Seah and Spencer[20], the attenuation A_{AB} of the photoelectrons from a deeper layer B through layer A is given by

$$A_{AB} = \exp\left(\frac{d_A}{\lambda_{AB}\cos\theta}\right) \tag{3.1}$$

Where d_A is the thickness of layer A, λ_{AB} is the attenuation length of the photoelectrons from layer B through layer A and $\cos\theta$ is the angle between the surface normal and the detection angle. That angle is always 90° in our case. The attenuation length is given by [21]

$$\lambda_{AB} = 0.316\sqrt{N_A}\left(\frac{E_B}{(Z_A)^{0.45}\ln(E_B/27)+3}+4\right) \tag{3.2}$$

Where N_A is the atomic density of A, E_B is the kinetic energy of the photoelectrons from B and Z_A is the average atomic number of layer A.

The production of photoelectrons in a thin layer is given by

$$I_A = I_{A\infty}(1-A_{AA}) = I_{A\infty}\left[1-\exp\left(\frac{d_A}{\lambda_{AA}}\right)\right] \tag{3.3}$$

Our sample consists of a NiAl bulk support, followed by a AlO_x interface and and one or two AlO_y surface layers. Using the equations above that leads to:

$$I_s = I_{s\infty}(1-A_{ss}) = I_{s\infty}\left[1-\exp\left(\frac{d_s}{\lambda_{ss}}\right)\right] \tag{3.4}$$

$$I_i = I_{i\infty}(1-A_{ii})A_{si} = I_{i\infty}\left[1-\exp\left(\frac{d_i}{\lambda_{ii}}\right)\right]\exp\left(\frac{d_s}{\lambda_{si}}\right) \tag{3.5}$$

$$I_b = I_{b\infty}A_{ib}A_{sb} = I_{b\infty}\exp\left(\frac{d_i}{\lambda_{ib}}\right)\exp\left(\frac{d_s}{\lambda_{sb}}\right) \tag{3.6}$$

where s is the surface layer, i the interface layer and b the bulk support.

In most XPS thickness calculations, one would now derive d_s from a combination of these equations. In such a case one assumes that the film homogeneously thick across the sample. For thicker films that assumption is valid, the film grows faster at thinner parts, so this self-correcting effect

will create a film of homogeneous thickness. But when a film is only 2 or 3 layers thick, as it is in our case, even the smallest change gives a 50% increase, which renders this assumption invalid.

Being unable to use this standard approach, we decided to make our own model. From the theory we know that it is much harder to grow oxide on a 3 layer film than it is on a 2 layer film. When we anneal enough we will only grow one layer at the time. This allows us to create a two level model, where α is the part of surface covered with 3 layers, and $1-\alpha$ is the part covered with 2 layers. Using that gives

$$\begin{aligned} I_s = \alpha I_{s3l} + (1-\alpha) I_{s2l} = \\ I_{s\infty}\alpha\left[1-\exp\left(\frac{2d_s}{\lambda_{ss}}\right)\right] + I_{s\infty}(1-\alpha)\left[1-\exp\left(\frac{d_s}{\lambda_{ss}}\right)\right] = \\ I_{s\infty}\alpha(1-A_{ss}^2) + I_{s\infty}(1-\alpha)(1-A_{ss}) = \\ I_{s\infty}[1-\alpha A_{ss}^2 - (1-\alpha)A_{ss}] \end{aligned} \tag{3.7}$$

$$\begin{aligned} I_i = \alpha I_{i3l} + (1-\alpha) I_{i2l} = \\ I_{i\infty}\left[1-\exp\left(\frac{d_i}{\lambda_{ii}}\right)\right]\left[\alpha\exp\left(\frac{2d_s}{\lambda_{si}}\right) + (1-\alpha)\exp\left(\frac{d_s}{\lambda_{si}}\right)\right] = \\ I_{i\infty}(1-A_{ii})(\alpha A_{si}^2 + (1-\alpha)A_{si}) \end{aligned} \tag{3.8}$$

$$\begin{aligned} I_b = \alpha I_{b3l} + (1-\alpha) I_{b2l} = \\ I_{b\infty}\exp\left(\frac{d_i}{\lambda_{ib}}\right)\left[\alpha\exp\left(\frac{2d_s}{\lambda_{sb}}\right) + (1-\alpha)\exp\left(\frac{d_s}{\lambda_{sb}}\right)\right] = \\ I_{b\infty}A_{ib}(\alpha A_{sb}^2 + (1-\alpha)A_{sb}) \end{aligned} \tag{3.9}$$

With the average film thickness being

$$\begin{aligned} d_{avg} = d_{3l}\alpha + d_{2l}(1-\alpha) = \\ (2d_s + d_i)\alpha + (d_s + d_i)(1-\alpha) = (d_s + d_i) + d_s\alpha \end{aligned} \tag{3.10}$$

To get the average thickness we need to solve (3.7), (3.8) and (3.9) for α. The easiest way to do so is by taking the Al2p peaks, since the bulk, interface and surface are three different peaks there. However, as we have shown in section 3.4 it is hard to get the fitting for the surface and interface peaks right, since they overlap so much. We therefore decided to use the O1s peaks.

Given the fact that the 2 different O1s peaks do not relate directly to two different layers [19], we can not use both peaks individually for the

thickness calculation, like we could for the Al2p peaks. We need to use their sum I_t and extract the surface and interface signals from there.

$$\frac{I_t}{I_b} = \frac{I_s + I_i}{I_b} = \frac{\frac{I_{s\infty}}{I_{b\infty}}[1 - \alpha A_{ss}^2 - (1-\alpha)A_{ss}] + \frac{I_{i\infty}}{I_{b\infty}}(1 - A_{ii})[\alpha A_{si}^2 + (1-\alpha)A_{si}]}{A_{ib}[\alpha A_{sb}^2 + (1-\alpha)A_{sb}]} \tag{3.11}$$

$$\frac{I_t}{I_b} A_{ib}[\alpha A_{sb}^2 + (1-\alpha)A_{sb}] = \frac{I_{s\infty}}{I_{b\infty}}[1 - \alpha A_{ss}^2 - (1-\alpha)A_{ss}] + \frac{I_{i\infty}}{I_{b\infty}}(1 - A_{ii})[\alpha A_{si}^2 + (1-\alpha)A_{si}] \tag{3.12}$$

Since we want to solve this equation for α we move them all to one side to extract α:

$$\alpha \left[\frac{I_t}{I_b} A_{ib}(A_{sb}^2 - A_{sb}) + \frac{I_{f\infty}}{I_{b\infty}}(A_{ss}^2 - A_{ss}) - \frac{I_{i\infty}}{I_{b\infty}}(1 - A_{ii})(A_{si}^2 - A_{si}) \right] = -\frac{I_t}{I_b} A_{ib} A_{sb} + \frac{I_{s\infty}}{I_{b\infty}}(1 - A_{ss}) + \frac{I_{i\infty}}{I_{b\infty}}(1 - A_{ii})A_{si} \tag{3.13}$$

$$\alpha = \frac{-\frac{I_t}{I_b} A_{ib} A_{sb} + \frac{I_{s\infty}}{I_{b\infty}}(1 - A_{ss}) + \frac{I_{i\infty}}{I_{b\infty}}(1 - A_{ii})A_{si}}{\frac{I_t}{I_b} A_{ib}(A_{sb}^2 - A_{sb}) + \frac{I_{s\infty}}{I_{b\infty}}(A_{ss}^2 - A_{ss}) - \frac{I_{i\infty}}{I_{b\infty}}(1 - A_{ii})(A_{si}^2 - A_{si})} \tag{3.14}$$

This formula can be used directly if $I_{b\infty}$, $I_{s\infty}$ and $I_{i\infty}$ are known. In the case of thin films this is impossible, since the thick films have a different crystal structure, and therefore a different I_∞. We can however calculate the ratios between the different intensities [22]:

$$\frac{I_{A\infty}}{I_{B\infty}} = \frac{N'_A \sigma_A \lambda_{AA} T_A}{N'_B \sigma_B \lambda_{BB} T_B} \tag{3.15}$$

Where N' is the atomic density of the element, σ is the photoionization cross section, which is a sensitivity factor, λ is the attenuation length, and T is the transmission function. Note that this N' is different than the N from equation 3.2. In that equation the total number of atoms per unit

volume is used, while here we only count the atoms of the element whose signal we measure.

$$\alpha = \frac{-\frac{I_t}{I_b}A_{ib}A_{sb} + \frac{N'_s\sigma_s\lambda_{ss}T_s}{N'_b\sigma_b\lambda_{bb}T_b}(1-A_{ss}) + \frac{N'_i\sigma_i\lambda_{ii}T_i}{N'_b\sigma_b\lambda_{bb}T_b}(1-A_{ii})A_{si}}{\frac{I_t}{I_b}A_{ib}(A_{sb}^2 - A_{sb}) + \frac{N'_s\sigma_s\lambda_{ss}T_s}{N'_b\sigma_b\lambda_{bb}T_b}(A_{ss}^2 - A_{ss}) - \frac{N'_i\sigma_i\lambda_{ii}T_i}{N'_b\sigma_b\lambda_{bb}T_b}(1-A_{ii})(A_{si}^2 - A_{si})} \tag{3.16}$$

Since the interface layer and surface layer signal are at the same energy, $\sigma_i = \sigma_s = \sigma_t$, $\lambda_{ii} = \lambda_{ss} = \lambda_{tt}$ and $T_i = T_s = T_t$.

$$\begin{aligned}\alpha &= \frac{-\frac{I_t}{I_b}\frac{N'_b\sigma_b\lambda_{bb}T_b}{\sigma_t\lambda_{tt}T_t}A_{ib}A_{sb} + N'_s(1-A_{ss}) + N'_i(1-A_{ii})A_{si}}{\frac{I_t}{I_b}\frac{N'_b\sigma_b\lambda_{bb}T_b}{\sigma_t\lambda_{tt}T_t}A_{ib}(A_{sb}^2 - A_{sb}) + N'_s(A_{ss}^2 - A_{ss}) - N'_i(1-A_{ii})(A_{si}^2 - A_{si})} \\ &= \frac{-\frac{I'_t}{I'_b}N'_bA_{ib}A_{sb} + N'_s(1-A_{ss}) + N'_i(1-A_{ii})A_{si}}{\frac{I'_t}{I'_b}N'_bA_{ib}(A_{sb}^2 - A_{sb}) + N'_s(A_{ss}^2 - A_{ss}) - N'_i(1-A_{ii})(A_{si}^2 - A_{si})}\end{aligned} \tag{3.17}$$

where $I'_A = \frac{I_A}{\sigma_A\lambda_{AA}T_A}$ is the corrected intensity. Our XPS software already calculates $\frac{I_A}{\lambda_{AA}T_A}$, so if we want to calculate the corrected intensity we only need to know σ_A. Getting the right value for σ_A is hard. There are big discrepancies between experimental and theoretical data, and experimental data is in general only available for the main peak of each element. For the Nickel 2p peak, for example, we could not find any convincing data. Therefore we decided to use them as a fitting parameter.

We know that our substrate is 50% nickel and 50% aluminum, so $N_{Ni} = N_{Al}$. So the corrected intensity on a sample without film should be the same. So the corrected intensity ratio of a sample with film would simply be the ratio of the attenuation. For a two layer film that means

$$\frac{I'_{Ni}}{I'_{Al}} = \frac{A_{Ni,i}A_{Ni,s}}{A_{Al,i}A_{Al,s}} \approx 1.0005 \tag{3.18}$$

And for a three layer film we get

$$\frac{I'_{Ni}}{I'_{Al}} = \frac{A_{Ni,i}A_{Ni,s}^2}{A_{Al,i}A_{Al,s}^2} \approx 1.0008 \tag{3.19}$$

In both cases this factor is much smaller than the expected fitting errors, so we used $I'_{Ni} = I'_{Al}$. This allows us to average over all 13 measurements

at different thicknesses to average out the fitting errors. We can now use the definition of the corrected intensity to calculate the sensitivity factor

$$\frac{\sigma_{Ni}}{\sigma_{Al}} = \frac{I'_{Al}}{I'_{Ni}} \frac{\frac{I_{Ni}}{\lambda_{Ni,b}T_{Ni}}}{\frac{I_{Al}}{\lambda_{Al,b}T_{Al}}} \approx \frac{\frac{I_{Ni}}{\lambda_{Ni,b}T_{Ni}}}{\frac{I_{Al}}{\lambda_{Al,b}T_{Al}}} \tag{3.20}$$

Because the sensitivity factor depends mostly on the atomic number, we assumed that σ_{Al} is the same for all aluminum species we have. For σ_O we used the fact that $\alpha = 0$ when we only dosed with O_2. Since only the numerator can make α zero, this gives

$$0 = \alpha = -\frac{I_{t0}}{I_{b0}} A_{ib} A_{sb} + \frac{I_{s\infty}}{I_{b\infty}}(1 - A_{ss}) + \frac{I_{i\infty}}{I_{s\infty}}(1 - A_{ii}) A_{si} \tag{3.21}$$

Putting in equation 3.15 and rearranging gives

$$\frac{I_{t0}/(\lambda_O T_O)}{I_{b0}/(\lambda_{bb} T_b)} A_{ib} A_{sb} = \frac{N_s}{N_b}\frac{\sigma_O}{\sigma_b}(1 - A_{ss}) + \frac{N_i}{N_b}\frac{\sigma_O}{\sigma_b}(1 - A_{ii}) A_{si} \tag{3.22}$$

$$\frac{\sigma_O}{\sigma_b} = \frac{\frac{I_{t0}/(\lambda_O T_O)}{I_{b0}/(\lambda_{bb} T_b)} A_{ib} A_{sb}}{\frac{N_f}{N_b}(1 - A_{ff}) + \frac{N_i}{N_b}(1 - A_{ii}) A_{si}} \tag{3.23}$$

With the equations for the sensitivity factor we can calculate the corrected intensity $I'_A = \frac{I_A}{\sigma_A \lambda_{AA} T_A}$, which is the last quantity we needed to know in order to calculate the thickness using equation 3.17.

Chapter 4

Results and discussion

4.1 Crystal structure

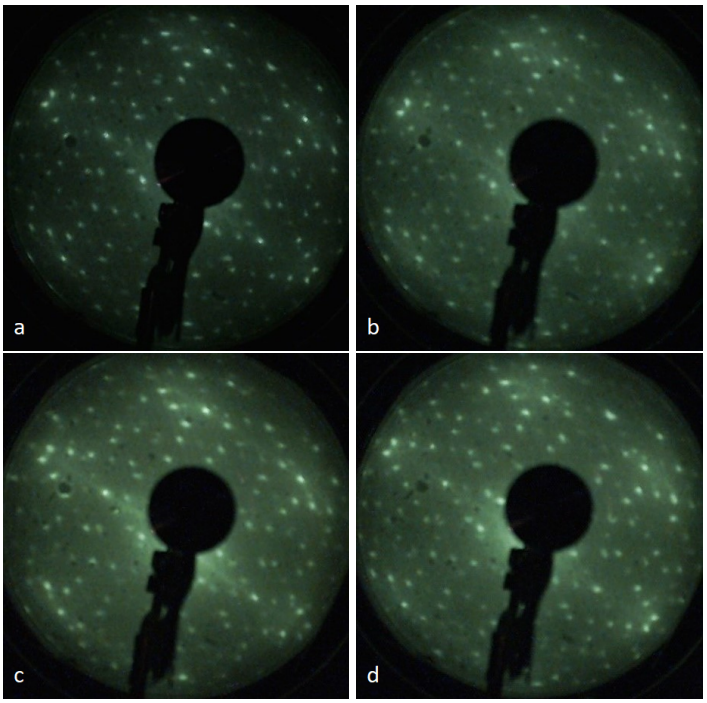

Figure 4.1: *LEED patterns of our surface, with a) 0 s of NO_2 oxidation, b) 2400 s of NO_2 oxidation, c) 4800 s of NO_2 oxidation and d) 6000 s of NO_2 oxidation.*

Low Energy Electron Diffraction is one of easiest way to see changes in the unit cell of the sample. After every two NO_2 cycles (600 s) we

have made a LEED measurement, and the results can be found in figure 4.1.When looking at those patterns the first thing we see is that there is very little change in the unit cell of the film. After 6000 s the unit cell is the same as the one we started with. Since we know that the unit cell did not change, we now also know that all unit cell related properties did not change, and that many literature sources are still valid, even for higher thicknesses. Comparing the LEED patterns with literature [23] does not show big changes either, which gives further evidence that we have created a crystalline film which remained crystalline when it becomes thicker.

When the sample is placed in the STM we can directly image the unit cell and compare it with said literature. On the top of the image there are clear rows about 1.5 to 2.0 nm wide. From Simon et al [5] we know the unit cell of the top oxide layer is 1.7 nm wide, so that fits well with our estimation.

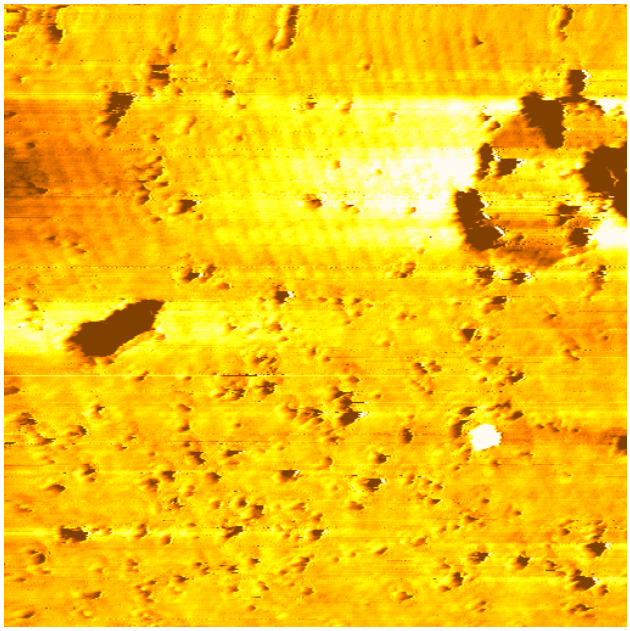

Figure 4.2: *STM image showing the size of the unit cell of our alumina film, which is between 1.5 nm and 2.0 nm wide. The image is 80 nm x 80 nm and taken in UHV conditions, with -1 V bias voltage and 100 pA tunneling current.*

When combining the results from the STM and the LEED with the cited literature sources, it is easy to conclude that our film has the same unit cell that has been reported numerous times for alumina on NiAl(110). Still unknown is the question whether or not the structure inside the unit cell changed. We simply did not have the STM resolution to either confirm or

reject that. But one could say that it would be very remarkable to have a change in crystal structure without a change in unit cell. Therefore we think it is save to say that the crystal structure did not change much, and that all the crystal structure related properties, did not change much either.

4.2 Film thickness

One of the main questions we wanted to answer asks about the increase of the oxide thickness due to the NO_2 oxidation. With the XPS data and equation (3.17) we can now calculate the thicknesses, which are shown in figure 4.3.

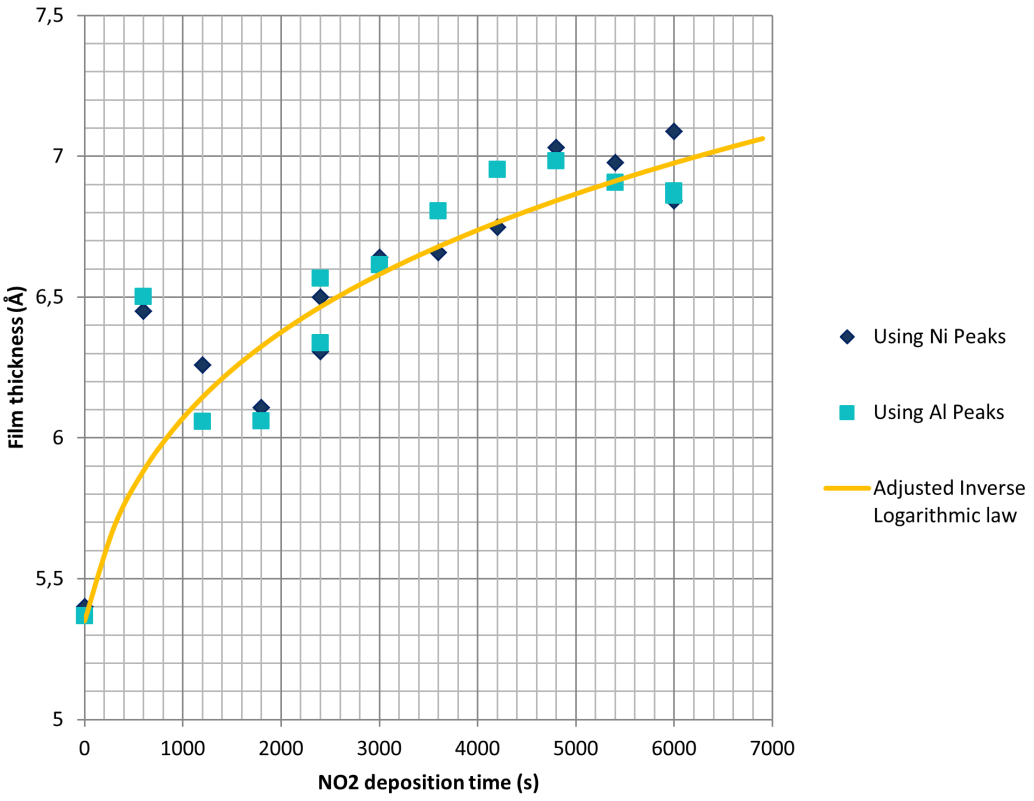

Figure 4.3: *The film thickness measurement, with equation* (2.10) *fitted with parameters* $X_1 = 62.9$ *Å,* $u = 1.68 \times 10^4$ *Å/s and* $\tau = 241$ *s. The point (0,5.35) is fixed as is done before in section 3.5, since that point is very well known from literature.*

At first it might look like the film thickness is decreasing after 4800 s of NO_2 oxidation. But that is most likely an error in measuring the size

of the peaks of the XPS spectrum. All literature says that extra NO_2 will increase the thickness of the film, or if the limit is reached stagnate the growth. To see whether or not that is true we would have to calculate the size of the measurement error. Unfortunately that is not possible. Not only does our fitting program not give any error information, there is also no direct fitting method. One has to assume the exact energy of the peaks and although they are generally known from literature, Popova et al [24] have shown that the the energy can increase or decrease based on film thickness. Beside this we also have the problem that the interface peak can not be resolved which shows that we have too little energy resolution to properly fit the peaks of this system.

This doesn't mean we can't learn anything from this data. One of the main achievements of the Cabrera Mott theory was the prediction of the film growth. Since we now have film growth data we wanted to test this prediction, by fitting our data in figure 4.3 to equation (2.10):

$$X = \frac{X_1}{2W_0\left(\sqrt{\frac{X_1}{4u(t+\tau)}}\right)}$$

Cabrera and Mott have given a range for the values of X_1 and u [2]. They say that X_1 should be between 100 Åand 1000 Å. This is larger than we have measured, but the error is less than an order of magnitude. Knowing the error margins in our data their range might very well be right. For u they do not give a fixed range, they only say that $u = u_0 \exp(-W/k_bT)$, where W is the potential energy of an diffusion location inside the film and $u_0 \sim 10^{12}$ Å/s or less. No information is available on W, so it is impossible to calculate u_0 for our case. The offset τ has been proposed by Ghez's adjustments to the original theory [3]. In his paper he eventually assumes τ to be very small and thus can be ignored, which works well for the cases he studies. In our case $\tau = 241$ s, which is big enough that it cannot be ignored. The reason for this lies in the method discussed in section 3.2. We first create a full 5.35 Åthick oxide film with O_2, before starting our NO_2 experiment. Therefore our timing is different from the case where one would start directly with NO_2, so it expected that τ could not be ignored.

Another remark has to be made with regards to the qualitative work of Baran et al [7] which is explained in section 2.2. They show why there is a limit, but don't give an equation for that limit if the exact reaction process is unknown, like it is for NO_2. Even in the cases they have studied themselves, they don't give an estimate on the thickness at which the Cabrera Mott theory starts to fail. Judging our own data does not give such a value

either. At 5400 s the fit fits perfectly to the data. One really needs to oxidize for a longer period or at a higher pressure in order to get such information.

4.3 Film growth location

Like we have explained in section 2.2 it is still unknown whether the alumina film grows at the surface or the interface. With our setup we should be able to distinguish the two. To do so a clean oxidized surface was scanned with STM, the dosed with 5×10^{-7} mbar NO_2 and scanned again, followed by being annealed at 1130 K. After two of those cycles we scanned again. The results are in figure 4.4.

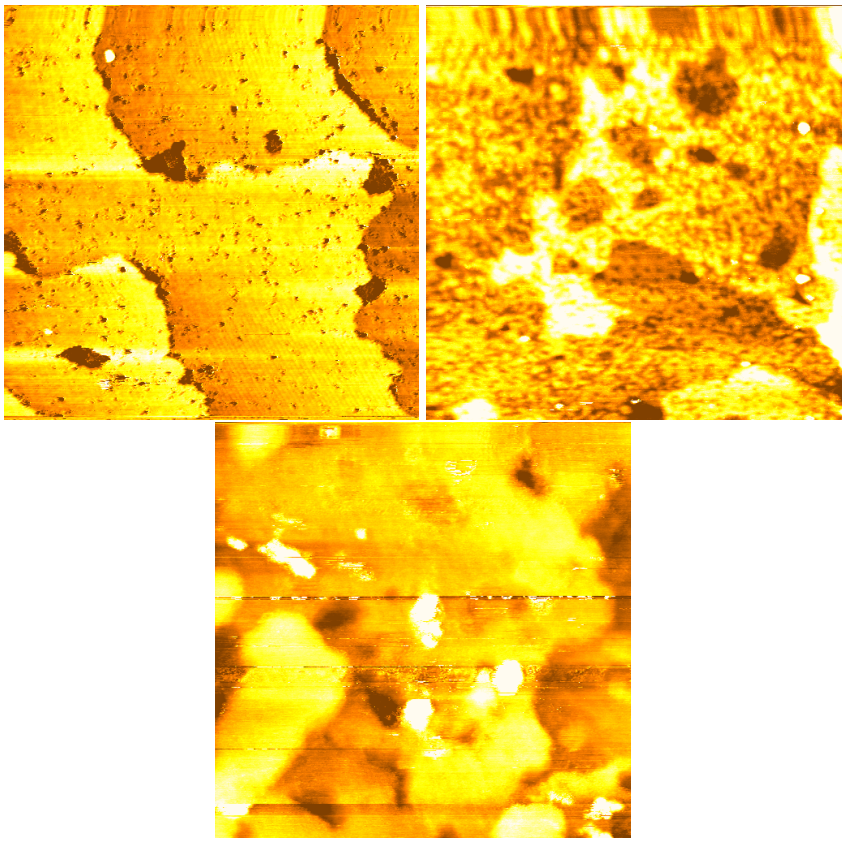

Figure 4.4: *STM images of our alumina on NiAl(110) sample before NO_2 oxidation (top left), after oxidation (top right) and after annealing and a second round of oxidation and annealing (bottom). All images are 80 nm x 80 nm and taken in UHV conditions, with -1 V bias voltage and 100 pA tunneling current.*

The first image is a control image. After we add NO_2 we see a large in-

crease in tiny islands, which means that those areas used to be conductive are now becoming insulating. NiAl is conductive and alumina insulating so NiAl is replaced by alumina, which means that the film grows at the interface. After annealing the small vacancy islands merge together, since that is more thermodynamically favorable and the annealing provides the thermal energy to do so.

4.4 Stability of MoO_3 nanoparticles

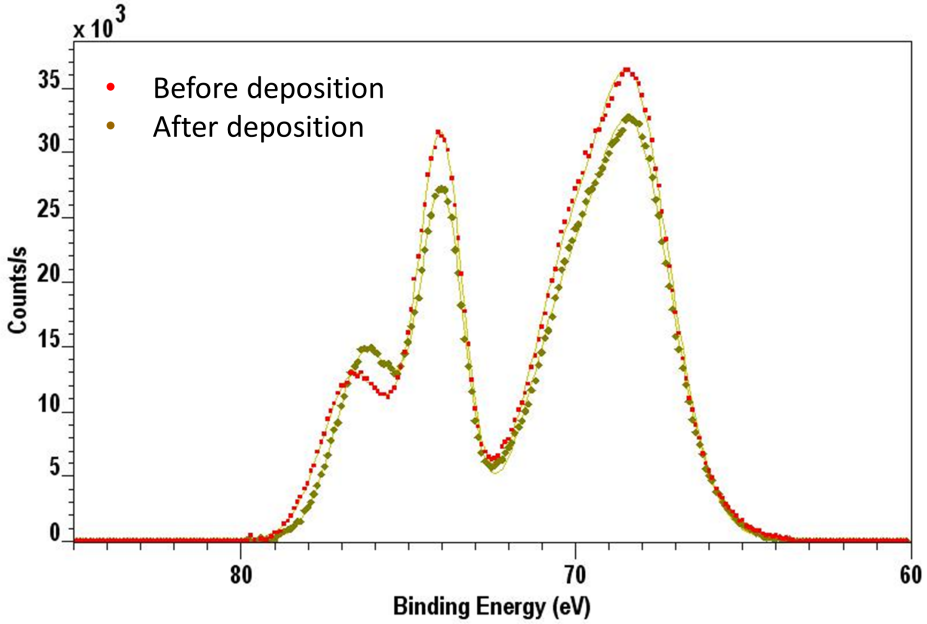

Figure 4.5: *After depositing the MoO_3 the aluminum and nickel bulk peaks have decreased, which shows that the film has grown. The alumina peak moved to a lower energy, indicating that the alumina film has changed in chemical composition.*

Now we know how the oxide film grows, what does and does not change, it is time to investigate the stability of MoO_3 nanoparticles on the thicker film. The average film thickness is measured before and after molybdenum oxide deposition. Before deposition the film had an average thickness of 6.9 Å, after deposition that is raised by 0.9 Åto 7.8 Å. One could argue that the film itself did not grow, since according to section 3.5 this measurement only uses the support and oxygen intensities. The support signal is attenuated by the molybdenum oxide nanoparticles like

it is by the alumina film, and both the film and the nanoparticles contain oxygen. We think this is incorrect, because of two reason. First, the aluminum bulk peak has decreased more than the nickel peak (-12.8% for the Al bulk peak versus -10.2% for the Ni bulk peak). This indicates that the top NiAl layer got deprived of aluminum. If the film grows at low temperatures, like we think has happened here, Cai et al [17] have shown that an aluminum deprived layer forms just beneath the film. Secondly, although it shifted so much in energy that our software could not fit the peak correctly, it is clear that the Al3+ peak itself grew. This could not have any other cause than the increase of the film thickness.

4.5 Carbon contamination

Carbon is one of the impurities in the NiAl crystal we have been using. As long as it stays away from the surface it does not influence the experiments. To measure whether is does or not, we used XPS. XPS is only sensitive in the top 10 nm of the sample, which is the film and the area just beneath it. Three times we have measured the Carbon XPS-signal, at the beginning, after 2400 s of NO_2 oxidation and after 6000 s of NO_2 oxidation, shown in figure 4.6. The results are unexpected: It looks like the first 2400 s of oxidation brought up more carbon near the surface, but the 3600 s of oxidation thereafter made it disappear.

To look for the cause we have to realize that there are two different processes at play here. One is the diffusion of the carbon through the sample. Under homogeneous conditions, the carbon atoms will diffuse and end up in a homogeneous uniform distribution. The second process is the chemical reaction between the surface oxygen and the bulk carbon atoms. The carbon atoms prefer to be at the surface because they can create carbon particles there. But even more energetically favorable is the creation of CO_2 gas. The carbon and oxygen atoms form CO_2 which is then pumped off by our system.

The limited amount of Carbon measured halfway through the experiment could be problematic. If they interfere with the film growth it could invalidate our results. But considering the fact that the carbon prefers the surface over the interface, which is where the film is growing, it is unlikely that it significantly interferes with the film growth. It is therefore not a concern with regards to our results.

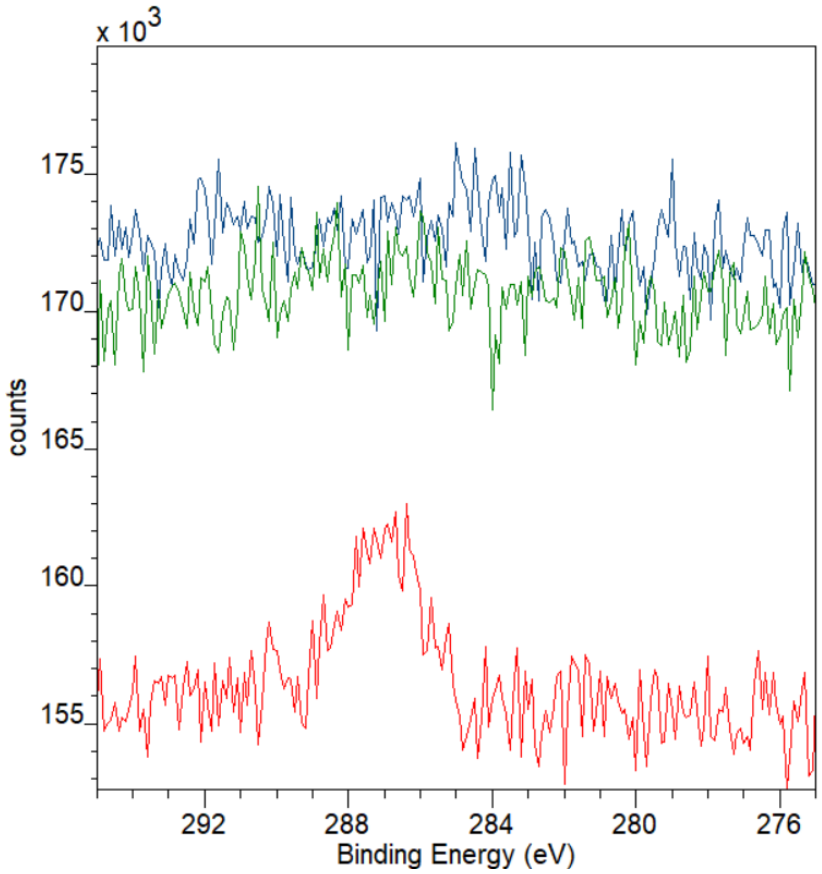

Figure 4.6: *XPS spectra of the C1s peak before NO_2 oxidation (blue), after 2400 s of NO_2 oxidation (red) and after 6000 s of NO_2 oxidation (green).*

Chapter 5

Conclusion

We have investigate the stepwise NO_2 oxidation of an alumina film on NiAl which has already been oxidized with O_2 up to 5.35Å, finding a thickness where MoO_3 nanoparticles are stable. The surface has been investigated every step with LEED, XPS and regularly STM as described in section 3.2.

Within the 11 LEED measurements performed we have seen very little change in the unit cell of the film. The LEED patterns and STM unit cell images correspond very well with the pattern and unit cell known from literature [1][5][23]. The crystal structure could not be observed directly, but it is very unlikely that the crystal structure changed without changing the unit cell. Using this fact we have shown that Ghez' adjustment [3] to the Cabrera-Mott theory [2], given by equation (2.10), is at least valid up to 6.9 Å. At that thickness the film still grew fast, as can be seen in figure 4.3. This shows that the thickness limit of NO2 oxidation, which predicted by Baran et al [7] as a hard limit, has not yet been reached.

Fitting of the thickness data has given us the values of the characteristic length $X_1 = 62.9$ Å, diffusion velocity $u = 1.68 \times 10^4$ Å/s and time offset $\tau = 241$ s. Although the errors on the data and the fit are big, they do correspond with the estimations given in the original article [2].

According to our measurement, the MoO_3 nanoparticles are still unstable on the thicker films. We deposited them on the 6.9 Åthick alumina film, which was the thickest film we could still scan on. Unfortunately, as one can see in figure 4.5 the MoO_3 nanoparticles were unstable and increased the film thickness from 6.9 Åto 7.8 Å. This all happened at low temperature, and all the low temperature effects described by Cai et al [17] have been recorded.

For the first time we have given clear experimental evidence of the lo-

cation of the oxide growth. STM images shown in figure 4.4 clearly show an increase in the number of conducting islands, which can only be explained if the oxide grows at the interface and not at the surface, since the alumina film is not conduct.

References

[1] G. Kresse, M. Schmid, E. Napetschnig, M. Shishkin, L. Köhler, and P. Varga, *Structure of the ultrathin aluminuium oxide film on NiAl(110) solved by STM and DFT.*, Science **1440** (2005).

[2] N. Cabrera and N. F. Mott, *Theory of the oxidation of metals*, Reports on Progress in Physics **12**, 163 (1949).

[3] R. Ghez, *On the Mott-Cabrera oxidation rate equation and the inverse-logarithmic law*, The Journal of Chemical Physics **58**, 1838 (1973).

[4] H. Freund, *Formation of a well-ordered by oxidation of NiAl (110)*, Surface and Interface Analysis **259**, 235 (1991).

[5] G. H. Simon, M. Heyde, and H.-J. Freund, *Imaging and manipulation of adatoms on an alumina surface by noncontact atomic force microscopy*, Journal of Physics: Condensed Matter **24**, 84007 (2012).

[6] R. V. Mom, M. J. Rost, J. W. Frenken, and I. M. Groot, *Tuning the Properties of Molybdenum Oxide on Al2O3/NiAl(110): Metal versus Oxide Deposition*, Journal of Physical Chemistry C **120**, 19737 (2016).

[7] J. D. Baran, H. Grönbeck, and A. Hellman, *Mechanism for limiting thickness of thin oxide films on aluminum*, Physical Review Letters **112**, 1 (2014).

[8] C. Ocal, S. Ferrer, and N. García, *Cabrera-Mott mechanism for oxidation of metals explains diffusion of metallic atoms through thin defective oxide layers*, Surface Science **163**, 335 (1985).

[9] N. Cai, G. Zhou, K. Müller, and D. E. Starr, *Tuning the limiting thickness of a thin oxide layer on Al(111) with oxygen gas pressure*, Physical Review Letters **107**, 1 (2011).

[10] I. Popova, V. Zhukov, and J. Yates, *Comparative study of Al(111) oxidation with O3 and O2*, Surface Science **518**, 39 (2002).

[11] T. T. Lay, M. Yoshitake, and W. Song, *Epitaxial growth of well-ordered ultra-thin Al2O3 film on NiAl (1 1 0) by a single-step oxidation*, Applied Surface Science **239**, 451 (2005).

[12] K. M. Ervin, J. Ho, and W. C. Lineberger, *Ultraviolet photoelectron spectrum of nitrite anion*, The Journal of Physical Chemistry **92**, 5405 (1988).

[13] M. J. Travers, D. C. Cowles, and G. Ellison, *Reinvestigation of the electron affinities of O2 and NO*, Chemical Physics Letters **164**, 449 (1989).

[14] C. T. Herbschleb, P. C. Van Der Tuijn, S. B. Roobol, V. Navarro, J. W. Bakker, Q. Liu, D. Stoltz, M. E. Cañas-Ventura, G. Verdoes, M. A. Van Spronsen, M. Bergman, L. Crama, I. Taminiau, A. Ofitserov, G. J. C. Van Baarle, and J. W. M. Frenken, *The ReactorSTM: Atomically resolved scanning tunneling microscopy under high-pressure, high-temperature catalytic reaction conditions*, Review of Scientific Instruments **85**, 083703 (2014).

[15] W. Song and M. Yoshitake, *Effects of surface cleaning on oxidation of NiAl(110)*, Applied Surface Science **241**, 164 (2005).

[16] M. Jaeger, H. Kuhlenbeck, J. Freund, M. Wuttig, W. Hoffmann, R. Franchy, and H. Ibach, *Formation of a well-ordered by oxidation of NiAl(110)*, Surface Science **259**, 235 (1991).

[17] N. Cai, H. Qin, X. Tong, and G. Zhou, *Growth of ultrathin amorphous alumina films during the oxidation of NiAl(100)*, Surface Science **618**, 20 (2013).

[18] A. Shavorskiy, K. Müller, J. T. Newberg, D. E. Starr, and H. Bluhm, *Hydroxylation of Ultrathin Al 2 O 3 /NiAl(110) Films at Environmental Humidity*, The Journal of Physical Chemistry C **118**, 29340 (2014).

[19] N. M. Martin, J. Knudsen, S. Blomberg, J. Gustafson, J. N. Andersen, and E. Lundgren, *High-resolution core-level spectroscopy study of the ultrathin aluminum oxide film on NiAl (110)*, Physical Review B **125417**, 1 (2011).

[20] M. P. Seah and S. J. Spencer, *Ultrathin SiO2 on Si IV. Intensity measurement in XPS and deduced thickness linearity*, Surface and Interface Analysis **35**, 515 (2003).

[21] P. J. Cumpson and M. P. Seah, *Elastic Scattering Corrections in AES and XPS. II. Estimating Attenuation Lengths and Conditions Required for their Valid Use in Overlayer/Substrate Experiments*, Surface and Interface Analysis **25**, 430 (1997).

[22] S. Hofmann, *Auger- and X-Ray Photoelectron Spectroscopy in Materials Science*, volume 49 of *Springer Series in Surface Sciences*, Springer, Berlin Heidelberg, 1 edition, 2013.

[23] J. Libuda, F. Winkelmann, M. Bäumer, H. J. Freund, T. Bertrams, H. Neddermeyer, and K. Müller, *Structure and defects of an ordered alumina film on NiAl(110)*, Surface Science **318**, 61 (1994).

[24] I. Popova, V. Zhukov, and J. Y. Jr, *Electrostatic field enhancement of Al (111) oxidation*, Physical review letters , 2 (2002).